



# Ammonia Ices Revisited: New IR Intensities and Optical Constants for Solid NH<sub>3</sub>

Reggie L. Hudson<sup>1</sup> , Perry A. Gerakines<sup>1</sup> , and Yukiko Y. Yarnall<sup>1,2</sup> <sup>1</sup> Astrochemistry Laboratory, NASA Goddard Space Flight Center, Greenbelt, MD 20771, USA; [reggie.hudson@nasa.gov](mailto:reggie.hudson@nasa.gov)<sup>2</sup> Universities Space Research Association, Greenbelt, MD 20771, USA

Received 2021 August 10; revised 2021 November 26; accepted 2021 November 27; published 2022 February 2

## Abstract

Solid ammonia (NH<sub>3</sub>) is the only nitrogen-containing polyatomic molecule reported in both interstellar and solar system ices. However, an examination of the literature reveals significant omissions and difficulties in earlier work that can hinder quantitative measurements of solid NH<sub>3</sub> by infrared (IR) methods by both astronomical observers and laboratory spectroscopists. Here we reinvestigate the IR spectra of NH<sub>3</sub> ices in amorphous and crystalline forms to determine mid- and near-IR intensities. The IR absorption coefficients, band strengths, and optical constants are presented for both amorphous and crystalline NH<sub>3</sub>, along with new density and refractive index ( $\lambda = 670$  nm) measurements needed to quantify our IR results. We find that two widely used approximate IR band strengths for amorphous NH<sub>3</sub> are nearly 30% higher than measured values after corrections for the compound's density. We have also used our new results to rescale two NH<sub>3</sub> near-IR band strengths in the literature, finding that they increase by about 60%. Some applications of our new results are described along with suggestions for future studies. Optical constants are available in electronic form.

*Unified Astronomy Thesaurus concepts:* [Molecular spectroscopy \(2095\)](#)

## 1. Introduction

Infrared (IR) spectroscopy remains the most reliable method for the remote identification of molecules and ions in extraterrestrial solids. Rotational spectroscopy is unsurpassed for gas-phase remote sensing, and mass spectrometry is invaluable for landers, rovers, and flybys, but IR spectroscopy remains the method of choice for the difficult task of identifying molecules in ices, whether interstellar or on solar system objects. As with many spectroscopic techniques, identifications involve comparing astronomical data to reference measurements from terrestrial laboratories. In some cases, it is possible not only to identify but also quantify IR detections to get molecular abundances. For the case of interstellar ices, an IR band is assigned to a specific molecule; it is then integrated and the result compared to the intrinsic IR band strength of that same feature, an approach that necessarily relies on reference band strengths measured in laboratories. The IR optical constants  $n(\tilde{\nu})$  and  $k(\tilde{\nu})$  are also used for identification and for compositional models of icy surfaces, particularly by planetary scientists, but again, lab work is required to generate such reference data.

To date, we have published IR band strengths, IR optical constants, or both for about 30 compounds in solid form. Our work has covered most of the common classes of organic molecules, such as hydrocarbons, alcohols, aldehydes, ketones, esters, ethers, thiols, and nitriles, plus a few inorganics, such as CO<sub>2</sub> and N<sub>2</sub>O. See Materese et al. (2021) for a complete list with references. Conspicuously absent from our work are saturated nitrogen-containing molecules such as ammonia (NH<sub>3</sub>) and amines. Therefore, in this paper, we continue our laboratory studies of IR spectral intensities by examining solid NH<sub>3</sub>, with results on amines planned for a separate paper.

The astrochemical relevance of NH<sub>3</sub> is easy to document. It was among the first interstellar molecules identified (Cheung et al. 1968), and it has since been found in comets (Altenhoff et al. 1983), in Jupiter's atmosphere (e.g., Owen 1970), and on Charon's surface (Brown & Calvin 2000). Ammonia is thought to have been present on the early Earth and was included in Miller's classic origin-of-life experiment (Miller 1953) and subsequent variations, such as the photolysis of icy solids to produce amino acids (Bernstein et al. 2002). Ammonia is also found in carbonaceous chondrite meteorites (Pizzarello & Williams 2012). Solid NH<sub>3</sub> is a component of interstellar ices (Lacy et al. 1998), with abundances of 3%–10% and a median of 6% relative to H<sub>2</sub>O ice (e.g., Gibb et al. 2004; Bottinelli et al. 2010; Boogert et al. 2015 and references therein). Ammonia is, in fact, the only nitrogen-containing molecule identified to date in interstellar ices, making its characterization particularly important. Frozen N<sub>2</sub> is reported in the solar system (e.g., Owen et al. 1993), and the cyanate ion OCN<sup>−</sup> has been identified in interstellar ices (e.g., Lacy et al. 1984), but neither species has been reported in both environments.

## 2. Previous Work on IR Intensities of NH<sub>3</sub>

Given the broad, long-standing astrochemical interest in NH<sub>3</sub>, it is not surprising that laboratory scientists have studied its solid forms in a variety of IR investigations. See Holt et al. (2004), for example, for a review of early IR spectroscopy of solid NH<sub>3</sub>. However, just as with astronomical observations, background IR reference data are needed to help quantify the laboratory measurements. Two types of investigations have been published: (1) those involving quantification using Beer's Law, optical constants, or both and (2) those based on an approximation of band intensities. We do not intend to review the history of the field, but a few published studies will be mentioned as representative. It will be seen that, somewhat surprisingly, one or more uncertainties accompany all of the earlier IR work with NH<sub>3</sub> ices.

An early report of the IR intensities of solid  $\text{NH}_3$  is from Robertson et al. (1975), who cooled liquid  $\text{NH}_3$  to prepare a crystalline ice of known thickness. The solid's IR spectrum was recorded at  $\sim 193$  K, and values of the apparent absorption coefficient ( $\alpha'$ ) were calculated at intervals of about  $10 \text{ cm}^{-1}$  or greater. From  $\alpha'$  values, optical constants  $k(\tilde{\nu})$  were derived using  $k(\tilde{\nu}) = \alpha'/(4\pi\tilde{\nu})$ , followed by calculation of  $n(\tilde{\nu})$  values with a Kramers–Kronig relationship and a reference refractive index (1.402 at  $\sim 2.08 \mu\text{m}$ ) based on a Lorentz–Lorenz value from liquid  $\text{NH}_3$ . Results were tabulated at intervals of  $10 \text{ cm}^{-1}$  and greater, a resolution far lower than that of the current work.

Later, Pipes et al. (1978) prepared crystalline  $\text{NH}_3$  by deposition of  $\text{NH}_3$  gas at a rate equivalent to an increase in the ice's thickness of  $\sim 100 \mu\text{m hr}^{-1}$ , based on a reference refractive index of 1.42 ( $\lambda = 633 \text{ nm}$ ). The deposition was at 80 K, which was also the temperature at which IR spectra were recorded. Spectra were analyzed with a Kramers–Kronig treatment to give optical constants  $n(\tilde{\nu})$  and  $k(\tilde{\nu})$ . Final results were again tabulated at intervals of  $10 \text{ cm}^{-1}$  and higher.

The IR intensity studies of Ferraro et al. (1980) and Sill et al. (1980) covered only crystalline  $\text{NH}_3$  at 88 K, producing optical constants, absorption coefficients ( $\alpha'$ ) of IR peaks, and apparent band strengths ( $A'$ ), but the lack of integration ranges hinders lab-to-lab comparisons.

For amorphous  $\text{NH}_3$ , there is the work of Zanchet et al. (2013), who studied  $\text{NH}_3$  near 10 K. Their paper included IR spectra, optical constants, and band strengths calculated from them. Integration ranges were given for mid-IR bands but not near-IR features. Moreover, one of the two largest mid-IR peaks severely overlapped with another feature, and the way they were separated, if they were, was not explained. An amorphous  $\text{NH}_3$  density from another lab was used for band strength calculations.

Bouilloud et al. (2015) reported IR band strengths of amorphous  $\text{NH}_3$  at 25 K in the mid-IR region. Their work was later used by Bergner et al. (2016) for an interesting study of interstellar acid–base chemistry. Unfortunately, Bouilloud et al. (2015) did not report the integration ranges needed for either accurate application of their IR intensities or lab-to-lab comparisons.

A much simpler approach to determining the IR intensities of  $\text{NH}_3$  was taken in an early study by d'Hendecourt & Allamandola (1986), who reported mid-IR band strengths for amorphous  $\text{NH}_3$  at 10 K based on an approximation to get IR band areas. Their  $\text{NH}_3$  band strengths have since been widely used to obtain IR intensities in other IR regions and quantify chemical reactions in ices. For example, Gálvez et al. (2010) and Förstel et al. (2017) cited d'Hendecourt & Allamandola (1986) for an  $\text{NH}_3$  band strength. Taban et al. (2003), Bossa et al. (2008), Pilling et al. (2010), and Lv et al. (2014) each used an  $\text{NH}_3$  band strength from Kerkhof et al. (1999), who, in turn, used the work of d'Hendecourt & Allamandola (1986). Jiménez-Escobar et al. (2014) and Giulano et al. (2014) both used the  $\text{NH}_3$  band strengths of Sandford & Allamandola (1993), which were based on d'Hendecourt & Allamandola (1986). Both Martín-Doménech et al. (2018) and Martín-Doménech et al. (2020) cited Schutte et al. (1996) for a band strength of  $\text{NH}_3$ , although apparently incorrectly, as no  $\text{NH}_3$  band strength is found there. The band strength used in each case seems to have been taken from d'Hendecourt & Allamandola (1986). Bottinelli et al. (2010) published an extensive survey of  $\text{NH}_3$  in ices around low-mass young stellar

objects, taking their  $\text{NH}_3$  band strength from Kerkhof et al. (1999), which was based on d'Hendecourt & Allamandola (1986), as already mentioned. The  $\text{NH}_3$  band strength used by both Gürtler et al. (2002) and Gibb et al. (2004) in their Infrared Space Observatory studies of interstellar  $\text{NH}_3$ -containing ices was also derived from the approximate values of d'Hendecourt & Allamandola (1986) and Kerkhof et al. (1999). Bouilloud et al. (2015) selected  $n$  and  $\rho$  values from a variety of literature sources and used them to analyze their laboratory IR spectra of amorphous  $\text{NH}_3$  at 25 K, comparing the results to, once more, the approximate band strengths of d'Hendecourt & Allamandola (1986).

Despite the extensive use of the d'Hendecourt & Allamandola (1986) results, several uncertainties exist concerning those authors' work. First, a density of  $1 \text{ g cm}^{-3}$  was assumed for amorphous  $\text{NH}_3$  as opposed to adopting a measured value, an assumption that directly influences the reported IR intensities. Second, no details were provided about the “laser interference technique” used to measure ice thicknesses. Third, the same paper refers to amorphous  $\text{NH}_3$ 's IR band shapes as “near Lorentzian” but presents an integration formula for a Gaussian curve, a change that alters the band strength and IR intensity by about 40% from that of a Lorentzian shape. It is also not clear if more than one ice sample was used to determine the two  $\text{NH}_3$  band strengths reported.

To summarize, earlier studies of solid  $\text{NH}_3$  suffer from multiple problems and concerns. These include questions about refractive index and density values (e.g., d'Hendecourt & Allamandola 1986; Zanchet et al. 2013), a lack of integration ranges (e.g., Bouilloud et al. 2015), questions about an integration formula (e.g., d'Hendecourt & Allamandola 1986), the low resolution of the published data (e.g., Robertson et al. 1975; Pipes et al. 1978), and a general lack of electronic versions of the spectra and optical constants. To address these problems, here we report new laboratory results to help quantify low-temperature IR studies and astronomical observations involving solid  $\text{NH}_3$  in interstellar and solar system environments. We consider two forms of  $\text{NH}_3$ , crystalline and noncrystalline (amorphous), and compare our results to previous work where possible. New measurements of the refractive indices and densities of  $\text{NH}_3$  ices are included to improve the quantification of our IR intensities. Spectra were measured for a range of ice thicknesses, extending slightly beyond the mid-IR region, and are at a higher spectral resolution than in most previous studies. Our results are presented graphically, in tables, and in electronic form.

### 3. Experimental Methods

Research-grade  $\text{NH}_3$  was purchased from Sigma Aldrich (now MilliporeSigma) and used as received.

Since the laboratory methods and procedures followed were identical to those described in several of our recent papers (e.g., Gerakines & Hudson 2020; Yarnall et al. 2020; Hudson et al. 2021), only a brief description is given here. Ice samples for IR studies were made by vapor-phase background deposition onto a precooled CsI substrate inside a vacuum chamber ( $\sim 10^8$  Torr) so as to give an increase in the resulting ice's thickness of a few microns per hour. Interference fringes recorded during ice growth gave each sample's thickness (*vide infra*), with values ranging from about 0.25 to  $16 \mu\text{m}$ . The IR spectra of the resulting ices were recorded in transmission from about 6000 to  $600 \text{ cm}^{-1}$ , baselines were straightened manually if needed, IR

**Table 1**  
Refractive Indices and Densities Measured<sup>a</sup>

Amorphous NH <sub>3</sub>		Crystalline NH <sub>3</sub>	
$n_{670}$	$\rho$ (g cm <sup>-3</sup> )	$n_{670}$	$\rho$ (g cm <sup>-3</sup> )
1.33	0.68	1.44	0.83

**Note.**

<sup>a</sup> Amorphous and crystalline ices were prepared and studied at 18 and 100 K, respectively. Values of  $n$  and  $\rho$  are averages of at least three measurements. Uncertainties are on the order of  $\pm 0.01$  and  $\pm 0.01$  g cm<sup>-3</sup> for  $n_{670}$  and  $\rho$ , respectively, and probably less. See the text.

bands were integrated, and peak heights were measured. Spectra were obtained with a resolution of 1 cm<sup>-1</sup>, typically with 100–200 scans per spectrum, always using a Thermo iS50 spectrometer with a DTGS detector. Checks were made to ensure that the features measured were neither resolution-limited nor saturated.

The thickness ( $h$ ) of each ice studied was determined with Equation (1) from Heavens (1955), where  $N_{\text{fr}}$  was the number of interference fringes recorded during ice formation,  $n$  was the ice’s refractive index at 670 nm, and  $\theta \approx 0^\circ$  was the angle between the incident laser beam and a line drawn perpendicular to the substrate:

$$h = \frac{N_{\text{fr}} \lambda}{2\sqrt{n^2 - \sin^2 \theta}}. \quad (1)$$

Our IR spectra are presented with a vertical scale of absorbance ( $\mathcal{A}$ ), defined according to Equation (2), where  $I_0$  and  $I$  are the intensities of the IR beam passing through the bare substrate alone and the substrate with the ice sample, respectively. The path length  $h$  of the beam through the ice is also, in our case, the ice’s thickness:

$$\mathcal{A} \equiv \log_{10} \left( \frac{I}{I_0} \right). \quad (2)$$

Apparent band strengths ( $A'$ ) and absorption coefficients ( $\alpha'$ ) for peaks were found with the Beer’s Law plots described by Equations (3) and (4):

$$\mathcal{A} = \left( \frac{\alpha'}{2.303} \right) h, \quad (3)$$

$$\int_{\text{band}} (\mathcal{A}) d\tilde{\nu} = \left( \frac{\rho_N A'}{2.303} \right) h. \quad (4)$$

In Equation (4),  $\rho_N$  is the number density calculated from a sample’s mass density ( $\rho$ ) using  $\rho_N = \rho (N_A/M)$ , where  $N_A$  is Avogadro’s constant and  $M$  is the compound’s molar mass. Graphs of the absorbance of IR peaks as a function of ice thickness were linear with slopes equal to  $(\alpha'/2.303)$ , from which  $\alpha'$  values were found according to Equation (3). Similarly, graphing band areas as a function of ice thickness gave linear plots from which, using Equation (4),  $A'$  values were calculated. An example of each type of graph is in the next section. See also Hollenberg & Dows (1961) for details. The factor of  $\ln(10) \approx 2.303$  in Equations (3) and (4) converts the common logarithmic scale (base 10) of most and perhaps all commercial IR spectrometers to the natural log scale (base e) often favored by astronomers who use optical depth ( $\tau$ ), where  $\tau = 2.303 \times \mathcal{A}$ , for IR observations. Throughout this paper,

we use  $\alpha'$  and  $A'$  to designate absorption coefficients and integrated band strengths, respectively, calculated from either an IR spectrum or optical constants  $n(\tilde{\nu})$  and  $k(\tilde{\nu})$ , reserving  $\alpha$  and  $A$  for absorption coefficients and band strengths calculated from optical constant  $k(\tilde{\nu})$  alone (Hudson et al. 2014a, 2014b).

Inspection of Equations (3) and (4) shows that their use requires the ice thickness ( $h$ ) to be measured, which, according to Equation (1), requires a reference index of refraction ( $n$ ). The latter was found in our lab through separate measurements with two-laser interferometry in a UHV chamber (background pressure  $\sim 10^{10}$  Torr) while, simultaneously, an INFICON quartz-crystal microbalance recorded the data with which we calculated each ice’s density ( $\rho$ ). See Hudson et al. (2017) for details. Since all lasers employed for thickness and  $n$  determinations had  $\lambda = 670$  nm, from here on, we use  $n_{670}$  to designate the visible-region refractive indices we measured. We note that the use of a UHV chamber to obtain  $n_{670}$  was scarcely worth the time and expense compared to the older equipment we used (e.g., Moore et al. 2010), but the only way we could measure ice densities was with our UHV setup’s microbalance.

Finally, we use the expression “Beer’s Law” for convenience, recognizing that several names are associated with this relation’s historical development (Pfeiffer & Liebafsky 1951; Malinin & Yoe 1961; Mayerhöfer et al. 2020).

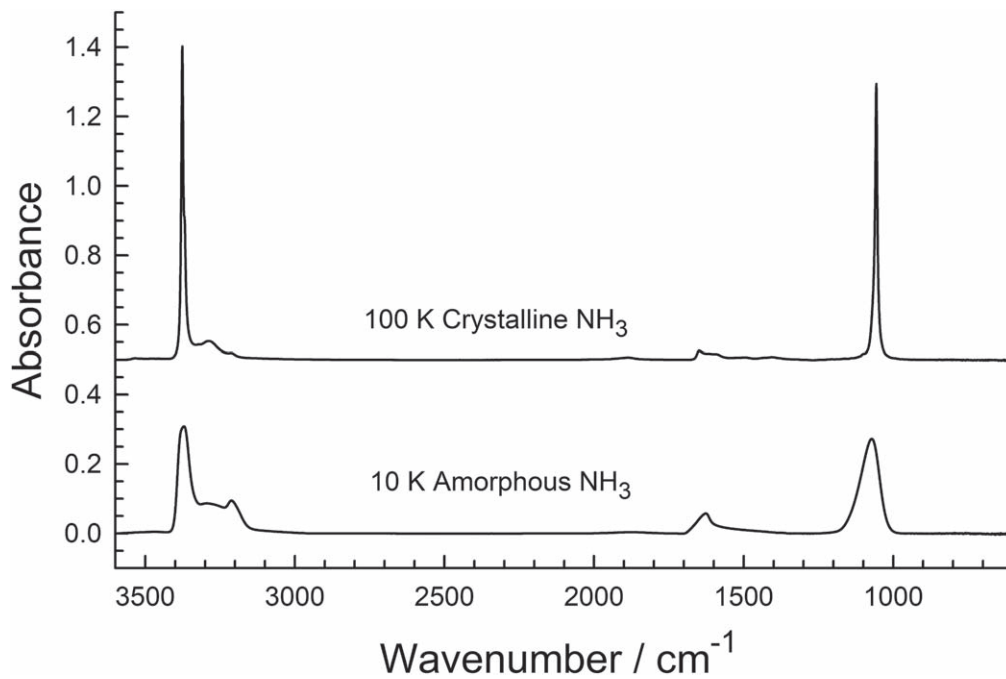
## 4. Results

Table 1 lists the refractive indices and densities we measured for NH<sub>3</sub> ices. At least three determinations of both  $n_{670}$  and  $\rho$  were made for each property in each ice form with standard errors of 0.01 and 0.01 g cm<sup>-3</sup> or less, respectively, and usually near 0.005 and 0.005 g cm<sup>-3</sup>. As in our earlier papers (e.g., Hudson et al. 2017, 2020), uncertainties in  $n_{670}$  and  $\rho$  are on the order of 1%, leading to uncertainties in  $\alpha'$  and  $A'$  on the order of 5%, and probably much lower.

Figures 1 and 2 show IR spectra of amorphous (10 K) and crystalline (100 K) NH<sub>3</sub> ices in the mid- and near-IR regions, respectively. Similar spectra of NH<sub>3</sub> can be found in the literature but not with the combination of two ice forms (amorphous and crystalline), spectral resolution and range, and direct measurements of  $n_{670}$  and  $\rho$  presented here. Examples of Beer’s Law plots are shown in Figure 3, displaying the linearity of the peak heights and band areas with thickness. We combined the slopes of such graphs with Equations (3) and (4) to calculate the IR absorption coefficients ( $\alpha'$ ) and band strengths ( $A'$ ) of Table 2.

An alternative to using  $\alpha'$  and  $A'$  for the IR intensities of ices involves the complex index of refraction,  $m(\tilde{\nu}) = n(\tilde{\nu}) - ik(\tilde{\nu})$ , with optical constants  $n(\tilde{\nu})$  and  $k(\tilde{\nu})$ . An advantage of IR optical constants over  $\alpha'$  and  $A'$  is that  $n(\tilde{\nu})$  and  $k(\tilde{\nu})$  can be used to generate the IR spectra of ices of various thicknesses. See Tomlin (1968) or Swanepoel (1983) for the relevant equations in algebraic form for calculating both transmission and reflection spectra.

We have presented our method for calculating optical constants in previous papers, the most detailed of which is Gerakines & Hudson (2020). There we describe an iterative process involving the Kramers–Kronig relation in which spectra of ices of known thickness can be used, in conjunction with a reference refractive index, to compute  $n(\tilde{\nu})$  and  $k(\tilde{\nu})$ . See Gerakines & Hudson (2020) for details, as well as our free, open-source software for the calculations.



**Figure 1.** Mid-IR baseline-corrected spectra of amorphous and crystalline  $\text{NH}_3$ . Each ice was made and its spectrum recorded at the temperature given in the figure. The amorphous ice had a thickness of about  $1 \mu\text{m}$ . The crystalline ice had a thickness of about  $0.5 \mu\text{m}$ . Spectra are offset vertically for clarity.

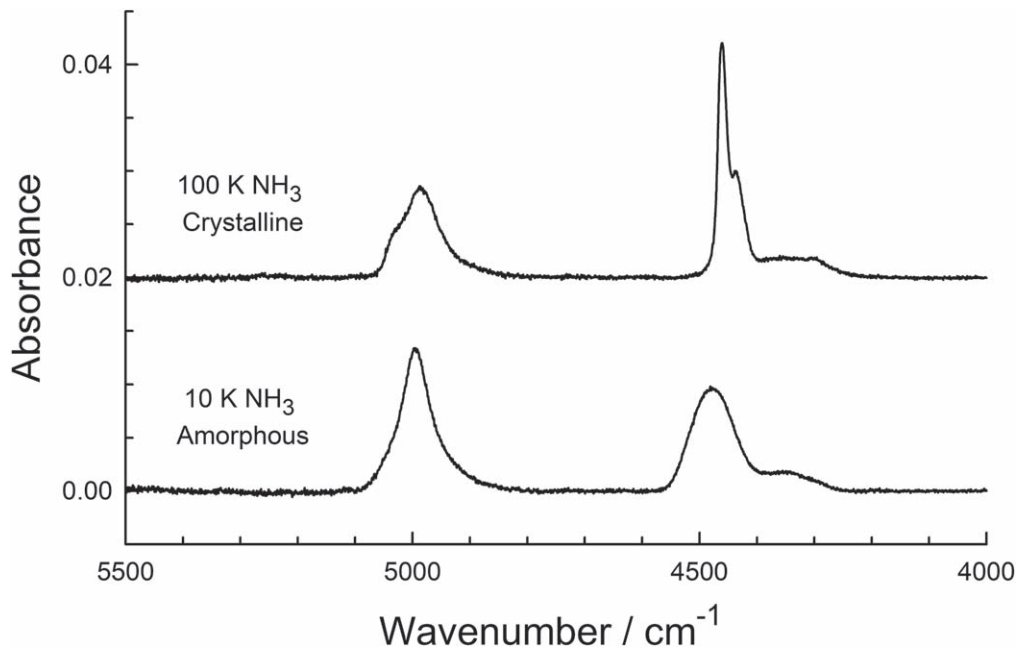


**Figure 2.** Near-IR baseline-corrected spectra of amorphous and crystalline  $\text{NH}_3$ . Each ice was made and its spectrum recorded at the temperature given in the figure. The amorphous ice had a thickness of about  $1 \mu\text{m}$ . The crystalline ice had a thickness of about  $0.5 \mu\text{m}$ . Spectra are offset vertically for clarity.

Figure 4 is an example of the optical constants we have calculated, those shown being for amorphous  $\text{NH}_3$  in the mid-IR region. All of our optical constants for  $\text{NH}_3$  ices are posted on our website, <https://science.gsfc.nasa.gov/691/cosmicice/constants.html>.

## 5. Discussion

### 5.1. Comparisons to Earlier Work

The refractive indices and densities of  $\text{NH}_3$  ices have been the focus of several studies, perhaps the most recent being from

Satorre et al. (2013). Their result for amorphous  $\text{NH}_3$  was  $n = 1.40$  at 20 K and 630 nm, compared to our  $n_{670} = 1.33$  at 18 K, a slightly lower temperature, giving  $n$  values almost within experimental error. For crystalline  $\text{NH}_3$  at 100 K, they obtained  $n = 1.48$  compared to our 1.44. Those same authors' densities for amorphous and crystalline  $\text{NH}_3$  were  $\rho = 0.72$  and  $0.85 \text{ g cm}^{-3}$ , respectively, close to ours in Table 1. The X-ray data of Olovsson & Templeton (1959) give  $\rho = 0.834 \text{ g cm}^{-3}$  at 171 K.

Qualitatively, the IR spectra in our figures are in good agreement with the transmission spectra we have found in the

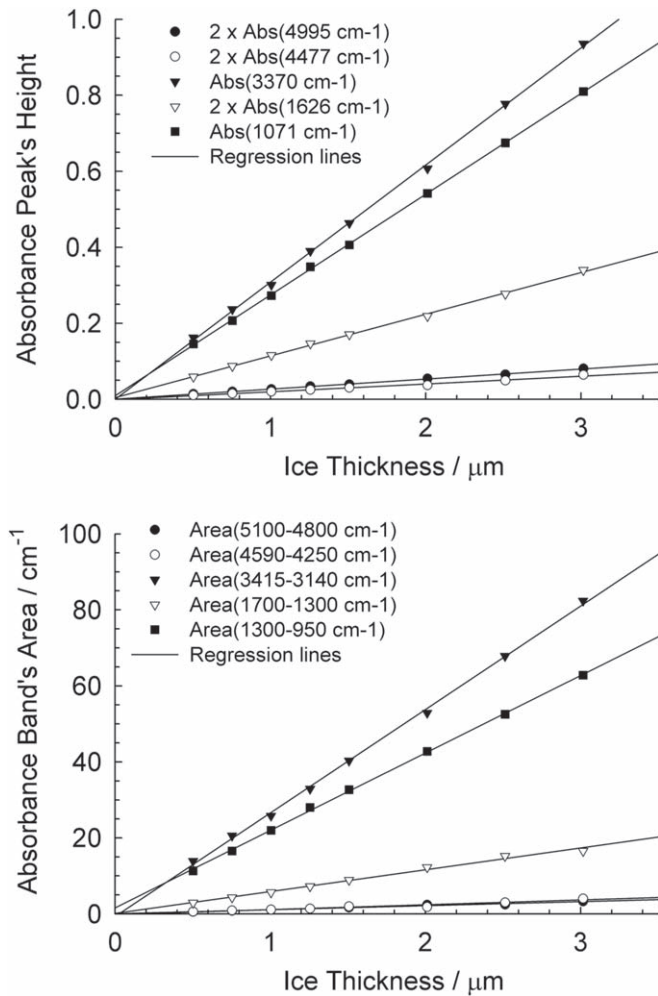


**Figure 3.** Beer's Law plots for five IR features of amorphous  $\text{NH}_3$ . Note that the absorbances of three features in the upper graph have been multiplied by 2 for clarity.

literature. For amorphous  $\text{NH}_3$ , see the spectrum of d'Hendecourt & Allamandola (1986), and for crystalline  $\text{NH}_3$ , there is the IR spectrum of Ferraro et al. (1980), among many others. In general, peak positions, bandwidths, and relative intensities are similar to those seen in our own figures. Readers interested in the details of the spectral assignments and the values of other peak positions should consult the papers just cited.

Quantitative comparisons of our work to the literature are much harder than qualitative ones for the reasons mentioned in Section 2, such as differences and uncertainties in sample preparation, spectral resolution, reference refractive indices, and ice densities. It also is unfortunate that comparisons remain difficult due to a lack of sharing of data, particularly in electronic form, and a lack of openness with software. Finally, accurate quantitative comparisons of IR band strengths are impossible in cases where integration ranges are not stated clearly or at all.

The best quantitative comparison we can make for our amorphous  $\text{NH}_3$  results is to data from Zanchet et al. (2013), who made their optical constants available in electronic form. We find reasonable agreement for relative IR intensities, particularly for the mid-IR region, but our band strengths are 20%–30% larger than the values of Zanchet et al. (2013). One reason for this disagreement is the difference in the  $k$  optical

**Table 2**  
Positions and Intensities of Selected IR Features of  $\text{NH}_3$  Ices

Assignment <sup>a</sup>	$\bar{\nu}/\text{cm}^{-1}$	$\alpha'/(\text{cm}^{-1})^b$	Integration Range ( $\text{cm}^{-1}$ )	$A'$ ( $10^{-18}$ cm molecule $^{-1}$ ) <sup>b</sup>
Amorphous $\text{NH}_3$ , 18 K				
$\nu_3 + \nu_4$	4995	303 <sup>c</sup>	5100–4800	1.3 <sup>c,d</sup>
$\nu_2 + \nu_3$	4477	237 <sup>c</sup>	4590–4250	1.4 <sup>c,d</sup>
$\nu_3$	3370	7090	3415–3140	26.1
$\nu_4$	1626	1260	1700–1300	5.50
$\nu_2$	1071	6100	1300–950	19.5
Crystalline $\text{NH}_3$ , 100 K				
$\nu_3 + \nu_4$	4986	426 <sup>c</sup>	5070–4800	1.25 <sup>c</sup>
$\nu_2 + \nu_3$	4461	1130 <sup>c</sup>	4500–4400	1.15 <sup>c</sup>
$\nu_3$	3376	50,800	3420–3150	31.2
$\nu_4$	1648	1400	1700–1265	5.49
$\nu_2$	1057	40,400	1200–900	21.6

**Notes.**

<sup>a</sup> Assignments of peaks are from Ferraro et al. (1980). Note that the integration range for  $\nu_3$  also covers the weaker  $\nu_1$  feature.

<sup>b</sup> Uncertainties in  $\alpha'$  and  $A'$  are  $\leq 5\%$ .

<sup>c</sup> The intensity results for these two weak near-IR features are considered somewhat less accurate than those for the mid-IR bands.

<sup>d</sup> See the Section 5 for these values, which were found by scaling from spectra with larger near-IR bands (Gerakines et al. 2005). Band strengths obtained in the present study without scaling were  $1.02 \times 10^{-18}$  and  $1.22 \times 10^{-18}$  cm molecule $^{-1}$  for the higher and lower wavenumber features, respectively.

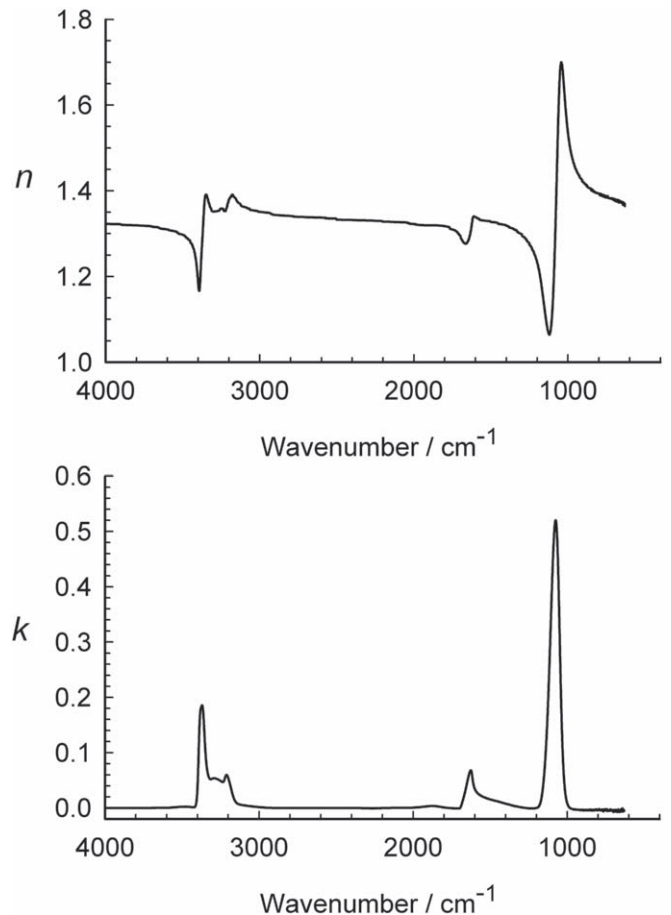


**Figure 4.** Optical constants of amorphous  $\text{NH}_3$  at 10 K.

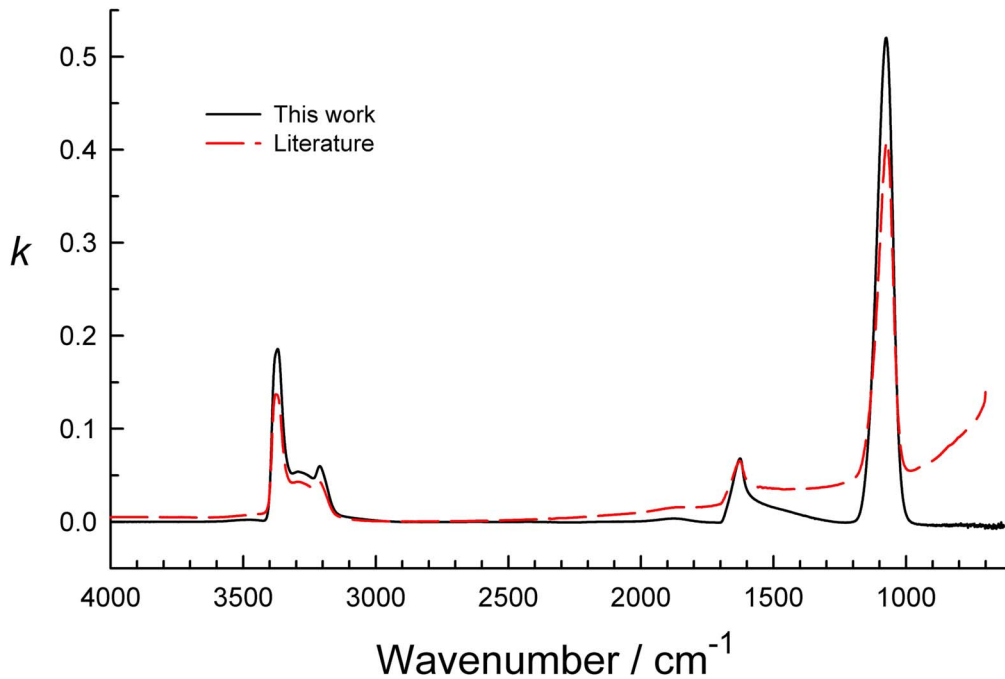


**Figure 5.** Optical constants  $k$  of amorphous  $\text{NH}_3$  at 10 K from this work (solid black line) compared to the  $k$  values of Zanchet et al. (2013) for amorphous  $\text{NH}_3$  at 15 K (dashed red line).

constants in the two sets of data, as seen in Figure 5. The reasons for the differences in  $k$  are unknown, but we suspect that one factor is that the literature spectrum has a baseline that is flat on the left and then shows a long rise from the middle of the spectrum and to the right. Also, Zanchet et al. (2013) used a slightly lower spectral resolution ( $2 \text{ cm}^{-1}$ ) than in our work ( $1 \text{ cm}^{-1}$ ), a different method to measure refractive indices, and a density taken from a different laboratory (Wood & Roux 1982). No integration ranges were given for the near-IR features of Zanchet et al. (2013), and the integral for one of the mid-IR features is not listed. Therefore, the only remaining comparison is to the amorphous  $\text{NH}_3$  band near  $1071 \text{ cm}^{-1}$ . Its band strength is about 30% below ours. Rescaling with our measured density reduces the difference to about 20%.

Turning to crystalline  $\text{NH}_3$ , the most complete IR intensity results we have found are those of Ferraro et al. (1980), who integrated spectral features, and Sill et al. (1980), who published absorption coefficients, both papers being for ices at 88 K. There is reasonable agreement between those authors' results and ours, although the lack of published integration ranges in Ferraro et al. (1980) makes precise comparisons of band strengths impossible. See our Table 3 and Figure 6 for comparisons of near-IR intensities. Note that the ratio of band strengths ( $A'$  values) for the near-IR features near 4986 and  $4461 \text{ cm}^{-1}$  is 1.10 in Ferraro et al. (1980) and 1.09 in our data, a good match. Similar comments and comparisons apply to the literature compilation of Martonchik et al. (1984), which is mainly drawn from the work of Sill, Ferraro, and associates. Howett et al. (2007) also studied crystalline  $\text{NH}_3$  at 80 K, but their published optical constants were for a smaller wavenumber range than both ours and that of Ferraro et al. (1980), a range that did not include either the intense  $\text{NH}_3$  feature near  $1057 \text{ cm}^{-1}$  or the near-IR peaks at  $4400\text{--}5000 \text{ cm}^{-1}$ . Moreover, detailed comparisons are difficult due to the  $10 \text{ cm}^{-1}$  separation between data points in their  $\text{NH}_3$  table. Similar comments apply to the older crystalline  $\text{NH}_3$  optical

**Table 3**  
Comparison of Selected IR Features of Crystalline  $\text{NH}_3$  Ices<sup>a</sup>

Approximate $\tilde{\nu}$ ( $\text{cm}^{-1}$ )	$\alpha'$ ( $\text{cm}^{-1}$ )		$A'$ ( $10^{-18} \text{ cm molecule}^{-1}$ )	
	This Work	Literature	This Work	Literature
4986	426	450	1.25	1.44
4461	1130	910	1.15	1.31
3376	50,800	45,000	31.2	32.0
1648	1400	1300	5.49	5.16
1057	40,400	40,000	21.6	20.9

**Note.**

<sup>a</sup> The integration ranges for our work are in Table 2 for crystalline  $\text{NH}_3$  at 100 K, and these were used to calculate  $A'$  from the literature results for  $\alpha'$  from Sill et al. (1980) and  $A'$  from Ferraro et al. (1980) for crystalline  $\text{NH}_3$  at 88 K.

constants of Pipes et al. (1978) and Wood & Roux (1982). In short, factors such as the coarseness of the published data, the lack of spectral range, the lower spectral resolution, and the lack of stated integration ranges hinder quantitative comparisons of our IR intensities of crystalline  $\text{NH}_3$  to earlier results.

### 5.2. Some Applications and Implications

We envision two main uses of our results by observational astronomers. First, the mid-IR band of amorphous  $\text{NH}_3$  near  $1071 \text{ cm}^{-1}$  ( $\lambda = 9.337 \mu\text{m}$ ) will probably continue to be used for observations of interstellar  $\text{NH}_3$  ices. To that end, we return to the long-used approximate band strengths of d'Hendecourt & Allamandola (1986) for amorphous  $\text{NH}_3$  values. For the  $\text{NH}_3$  feature near  $1070 \text{ cm}^{-1}$ , those authors reported  $A' = 1.7 \times 10^{-17} \text{ cm molecule}^{-1}$ , compared to our  $A' = 2.0 \times 10^{-17} \text{ cm molecule}^{-1}$ . For the  $3400\text{--}3100 \text{ cm}^{-1}$  region of amorphous  $\text{NH}_3$ , those authors' approximation gave  $A' = 2.2 \times 10^{-17} \text{ cm molecule}^{-1}$  compared to our  $A' = 2.6 \times 10^{-17} \text{ cm molecule}^{-1}$ . In each case, the older approximate results are about 14% below our direct

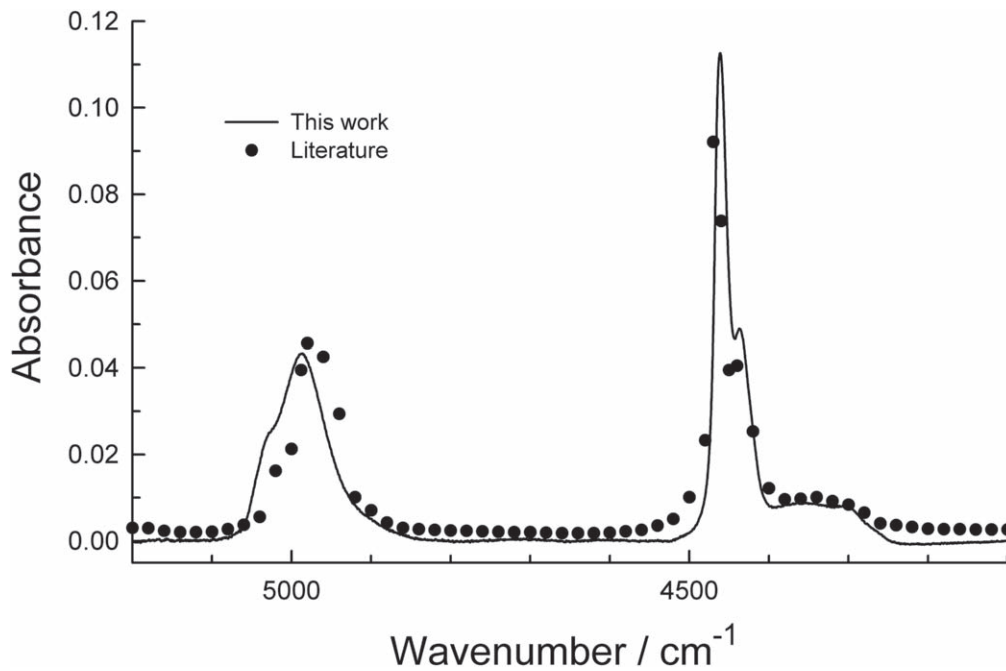


**Figure 6.** Near-IR spectrum of crystalline  $\text{NH}_3$  at 100 K from this work (solid line) overlaid with a spectrum (dots) calculated from the absorption coefficients of Sill et al. (1980) for an ice at 88 K. Both spectra are for an ice of thickness  $2.33 \mu\text{m}$ .

measurements (with similar differences with the results of Bouilloud et al. 2015). If the older results are rescaled using our measured ice density, then the approximations are about 26% higher than our measured values. We recommend the use of our new band strengths in Table 2 for amorphous  $\text{NH}_3$ .

Kerkhof et al. (1999) showed that for  $\text{NH}_3$ 's IR feature near  $1070 \text{ cm}^{-1}$ , the ratio of  $A'$  in amorphous  $\text{NH}_3$  to  $A'$  in an  $\text{H}_2\text{O}$ -rich mixture is about 0.75. With our value of  $A'(1070 \text{ cm}^{-1}) = 1.95 \times 10^{17} \text{ cm molecule}^{-1}$ , those authors' band strength for  $\text{NH}_3$  in  $\text{H}_2\text{O}$ -rich ices rises to  $\sim 1.5 \times 10^{17} \text{ cm molecule}^{-1}$ , an increase of about 15% over the value used by Bottinelli et al. (2010) in their study of  $\text{NH}_3$  in low-mass young stellar objects. Put another way, the  $A'$  value of d'Hendecourt & Allamandola (1986) for amorphous  $\text{NH}_3$  has to be lowered for  $\text{H}_2\text{O}$ -rich ices, but our density measurements cause the resulting band strength to be raised, resulting in a fortuitous near-cancellation of changes to the band strength. This small increase in  $A'(1070 \text{ cm}^{-1})$  implies that the reported  $\text{NH}_3$  abundances in young stellar objects have to be scaled down, but only slightly.

Another possible use of our data by observational astronomers involves the two IR bands of crystalline  $\text{NH}_3$  at  $5500\text{--}4000 \text{ cm}^{-1}$  ( $\lambda = 1.818\text{--}2.500 \mu\text{m}$ ), which are in the near-IR region often favored by planetary observers. We measured the IR intensities of these features, but better values come from using the thicker ices, and therefore stronger absorbances, of Gerakines et al. (2005). Those authors calculated the intensities of the same two bands of our Figure 2 by comparing to  $\text{NH}_3$ 's IR feature at  $1071 \text{ cm}^{-1}$ . Rescaling their work with our new  $A'(1071 \text{ cm}^{-1})$  gives  $A'(4995 \text{ cm}^{-1}) = 1.3 \times 10^{18}$  and  $A'(4477 \text{ cm}^{-1}) = 1.4 \times 10^{18} \text{ cm molecule}^{-1}$ , an increase in each case by about 60% over the older published results found indirectly by scaling (Gerakines et al. 2005). Table 2 gives the rescaled  $A'$  values of the two near-IR features of amorphous  $\text{NH}_3$  at  $5500\text{--}4000 \text{ cm}^{-1}$ . We also measured values of  $A'$  for these features using Beer's Law without scaling, as we did in the

cases of the strong mid-IR absorptions, but the areas involved are significantly smaller and therefore less reliable.

We should point out here that solvent effects in IR and other types of spectroscopy have been studied for well over a half-century, and it is known that such effects can lead to changes in an absorption band's shape, position, height, width, and area (e.g., Tsubomura 1955; Stephenson & Sponer 1957; Ritchie et al. 1962; Evans & Lo 1965). It would not be surprising, therefore, if the  $\text{NH}_3$ -ice results in Table 2 were altered by molecular interactions in  $\text{H}_2\text{O} + \text{NH}_3$  ice mixtures. However, we caution that the existence and extent of any such matrix effects for solid  $\text{NH}_3$  cannot be assumed a priori and can only be determined by laboratory work. Along these lines, we recently measured the IR band strength of the  $\text{C} \equiv \text{N}$  stretching vibration in solid HCN and found it to be essentially the same in the presence and absence of  $\text{H}_2\text{O}$  ice (Gerakines et al. 2022), with new determinations of  $n$  and  $\rho$  for HCN helping us to prepare ice mixtures of accurately known HCN abundances. A similar study of  $\text{H}_2\text{O} + \text{NH}_3$  ices could use our new results in Table 1 to prepare solid mixtures of accurately known  $\text{NH}_3$  abundances to investigate possible matrix effects. Band integrations in  $\text{H}_2\text{O}$ -rich ice mixtures could be more challenging for  $\text{NH}_3$  than for HCN due to the closer proximity of  $\text{NH}_3$ 's larger IR features to IR bands of  $\text{H}_2\text{O}$ .

A laboratory application of our results arises in the preparation of gas-phase mixtures for condensation to make mixed molecular ices, such as a  $\text{CO} + \text{NH}_3$  reactant mixture to make a cyanate ion ( $\text{OCN}$ ), perhaps by radiolysis or photolysis (Hudson et al. 2001). Ammonia's deposition rate can easily be quantified using our results in a deposition of pure (neat)  $\text{NH}_3$ . Improving the accuracy with which the starting material's abundance is known results in an improvement in calculations of the yields of products.

A nonlaboratory application concerns the need for a first-principles computational method to calculate solid-phase IR band strengths, especially for compounds that are difficult to obtain, particularly dangerous, or prohibitively expensive (e.g.,

HCN and C<sub>2</sub>N<sub>2</sub>). Sets of IR intensity measurements are needed to evaluate any such computational method. The results provided in this paper will contribute to such work.

## 6. Summary and Conclusions

This paper presents mid-IR band strengths and absorption coefficients, densities, and refractive indices for amorphous and crystalline NH<sub>3</sub> ices at astrophysically relevant temperatures, with IR results extending into the near-IR region. All data were measured in the same laboratory. Optical constants with a resolution of 1 cm<sup>-1</sup>, which is higher than in earlier published results, have been calculated and are available in electronic form.

Our results show that the approximate mid-IR band strengths of amorphous NH<sub>3</sub> published in and widely used since 1986 (d'Hendecourt & Allamandola 1986) are ~14% below the actual values. Corrections for amorphous NH<sub>3</sub>'s density give band strengths that are ~26% too large.




A near-cancellation of adjustments results in the published A' (1070 cm<sup>-1</sup>) band strengths of NH<sub>3</sub> in H<sub>2</sub>O-rich ices changing by only about 15%.

The published near-IR band strengths for two IR features of amorphous NH<sub>3</sub> at 5500–4000 cm<sup>-1</sup>, which were measured indirectly, have been rescaled in light of our new results, resulting in each feature's IR band strength rising by about 60%.

Although precise comparisons are difficult, the mid- and near-IR intensities reported here for crystalline NH<sub>3</sub> are in reasonable agreement with the literature results, which were obtained at a lower spectral resolution.

We acknowledge funding from NASA's Planetary Science Division Internal Scientist Funding Program through the Fundamental Laboratory Research (FLaRe) work package at the NASA Goddard Space Flight Center. Y.Y.Y. thanks the NASA Postdoctoral Program for her fellowship.

## ORCID iDs

Reggie L. Hudson  <https://orcid.org/0000-0003-0519-9429>  
 Perry A. Gerakines  <https://orcid.org/0000-0002-9667-5904>  
 Yukiko Y. Yarnall  <https://orcid.org/0000-0003-0277-9137>

## References

Altenhoff, W. J., Batrla, W. K., Huchtmeier, S. J., Stumpf, P., & Walmsley, W. 1983, *A&A*, **125**, L19  
 Bergner, J. B., Öberg, K. I., Rajappan, M., & Fayolle, E. C. 2016, *ApJ*, **829**, 1  
 Bernstein, M. P., Dworkin, J. P., Sandford, S. A., Cooper, G. W., & Allamandola, L. J. 2002, *Natur*, **416**, 401  
 Boogert, A. C. A., Gerakines, P. A., & Whittet, D. C. B. 2015, *ARA&A*, **53**, 541  
 Bossa, J. B., Theulé, P., Duvernay, F., Borget, F., & Chiavassa, T. 2008, *A&A*, **492**, 719  
 Bottinelli, S., Boogert, A. C. A., Bouwman, J., et al. 2010, *ApJ*, **718**, 1110  
 Bouilloud, M., Fray, N., Bénilan, Y., et al. 2015, *MNRAS*, **451**, 2145  
 Brown, M. E., & Calvin, W. M. 2000, *Sci*, **287**, 107  
 Cheung, A. C., Rank, D. M., Townes, C. H., Thornton, D. D., & Welch, W. J. 1968, *PhRvL*, **25**, 1701  
 d'Hendecourt, L. B., & Allamandola, L. J. 1986, *A&AS*, **64**, 453

Evans, H. C., & Lo, G. Y.-S. 1965, *JPhCh*, **69**, 3650  
 Ferraro, J. R., Sill, G., & Fink, U. 1980, *ApSpe*, **34**, 525  
 Förstel, M., Bergantini, A., Maksyutenko, P., Góbi, S., & Kaiser, R. I. 2017, *ApJ*, **845**, 1  
 Gálvez, O., Maté, N., Herrero, V. J., & Escribano, R. 2010, *ApJ*, **724**, 539  
 Gerakines, P. A., Bray, J. J., Davis, A., & Richey, C. 2005, *ApJ*, **620**, 1140  
 Gerakines, P. A., & Hudson, R. L. 2020, *ApJ*, **901**, 1  
 Gerakines, P. A., Yarnall, Y. Y., & Hudson, R. L. 2022, *MNRAS*, **509**, 3515  
 Gibb, E. L., Whittet, D. C. B., Boogert, A. C. A., & Tielens, A. G. G. M. 2004, *ApJSS*, **151**, 35  
 Giulano, B. M., Escribano, R. M., Martín-Doménech, R., Dartois, E., & Muñoz Caro, G. M. 2014, *A&A*, **565**, A108  
 Gürtler, J., Klaas, U., Henning, T., et al. 2002, *A&A*, **390**, 1075  
 Heavens, O. S. 1955, *Optical Properties of Thin Solid Films* (2nd edn; New York: Dover), 114  
 Hollenberg, J. L., & Dows, D. A. 1961, *JChPh*, **34**, 1061  
 Holt, J. S., Sadoskas, D., & Pursell, C. J. 2004, *JChPh*, **120**, 7153  
 Howett, C. J. A., Carlson, R. W., Irwin, P. G. J., & Calcutt, S. B. 2007, *JOSAB*, **24**, 126  
 Hudson, R. L., Ferrante, R. F., & Moore, M. H. 2014a, *Icar*, **228**, 276  
 Hudson, R. L., Gerakines, P. A., & Moore, M. H. 2014b, *Icar*, **243**, 148  
 Hudson, R. L., Loeffler, M. J., Ferrante, R. F., Gerakines, P. A., & Coleman, F. M. 2020, *ApJ*, **891**, 1  
 Hudson, R. L., Loeffler, M. J., & Gerakines, P. A. 2017, *JChPh*, **146**, 0243304  
 Hudson, R. L., Moore, M. H., & Gerakines, P. A. 2001, *ApJ*, **550**, 1140  
 Hudson, R. L., Yarnall, Y. Y., Gerakines, P. A., & Coones, R. T. 2021, *Icar*, **354**, 14033  
 Jiménez-Escobar, A., Giuliano, B. M., Muñoz Caro, G. M., Cernicharo, J., & Marcelino, N. 2014, *ApJ*, **788**, 1  
 Kerkhof, O., Schutte, W. A., & Ehrenfreund, P. 1999, *A&A*, **346**, 990  
 Lacy, J. H., Baas, F., Allamandola, L. J., et al. 1984, *ApJ*, **276**, 533  
 Lacy, J. H., Faraji, H., Sandford, S. A., & Allamandola, L. J. 1998, *ApJL*, **501**, L105  
 Satorre, M. Á., Leliwa-Kopystynski, J., Santonja, C., & Luna, R. 2013, *Icar*, **225**, 703  
 Lv, X. Y., Boduch, P., Ding, J. J., et al. 2014, *PCCP*, **16**, 3433  
 Malinin, D. R., & Yoe, J. H. 1961, *JChEd*, **38**, 129  
 Martín-Doménech, R., Cruz-Díaz, G. A., & Muñoz Caro, G. M. 2018, *MNRAS*, **473**, 2575  
 Martín-Doménech, R., Öberg, K. I., & Rajappan, M. 2020, *ApJ*, **894**, 1  
 Martonchik, J. V., Orton, G. S., & Appleby, J. F. 1984, *ApOpt*, **23**, 541  
 Materese, C. K., Gerakines, P. A., & Hudson, R. L. 2021, *AcChR*, **54**, 280  
 Mayerhöfer, T. G., Pahlow, S., & Popp, J. 2020, *ChemPhysChem*, **21**, 2029  
 Miller, S. L. 1953, *Sci*, **117**, 528  
 Moore, M. H., Ferrante, R. F., Moore, W. J., & Hudson, R. 2010, *ApJS*, **191**, 96  
 Olovsson, I., & Templeton, D. H. 1959, *Acta Cryst*, **12**, 832  
 Owen, T. 1970, *Sci*, **167**, 1675  
 Owen, T. C., Roush, T. L., Cruikshank, D. P., et al. 1993, *Sci*, **261**, 745  
 Pfeiffer, H. G., & Liebhafsky, H. A. 1951, *JChEd*, **28**, 123  
 Pilling, S., Seperuelo Duarte, E., da Silveira, E. F., et al. 2010, *A&A*, **509**, A87  
 Pipes, J. G., Roux, J. A., Smith, A. M., & Scott, H. E. 1978, *AIAAJ*, **16**, 984  
 Pizzarello, S., & Williams, L. B. 2012, *ApJ*, **749**, 1  
 Ritchie, C. D., Honour, R. J., & Bierl, B. A. 1962, *JChS*, **84**, 4687  
 Robertson, C. W., Downing, H. D., Curmutte, B., & Williams, D. 1975, *JOSA*, **65**, 432  
 Sandford, S. A., & Allamandola, L. J. 1993, *ApJ*, **417**, 815  
 Schutte, W. A., Gerakines, P. A., Geballe, T. R., van Dishoeck, E. F., & Greenberg, J. M. 1996, *A&A*, **309**, 633  
 Sill, G., Fink, U., & Ferraro, J. R. 1980, *JOSA*, **70**, 724  
 Stephenson, H. P., & Sponer, H. 1957, *JChS*, **79**, 2050  
 Swanepoel, R. 1983, *JPhE*, **16**, 1214  
 Taban, I. M., Schutte, W. A., Pontoppidan, K. M., & van Dishoeck, E. F. 2003, *A&A*, **399**, 169  
 Tomlin, S. G. 1968, *BJAP*, **2**, 1667  
 Tsubomura, H. 1955, *JChPh*, **23**, 2130  
 Wood, B. E., & Roux, J. A. 1982, *JOSA*, **72**, 720  
 Yarnall, Y. Y., Gerakines, P. A., & Hudson, R. L. 2020, *MNRAS*, **494**, 4606  
 Zanchet, A., Rodríguez-Lazcano, Y., Gálvez, Ó., et al. 2013, *ApJ*, **777**, 1